η^3-Edge-Bridging versus η^3-Face-Capping Coordination of a Conjugated Ynenyl Ligand on a Triruthenium Cluster Core

Javier A. Cabeza,*,† Ignacio del Río,† Santiago García-Granda,‡ Marta Moreno,† Enrique Pérez-Carreño,‡ and Marta Suárez†

Departamento de Química Orgánica e Inorgánica, Instituto de Química Organometálica "Enrique Moles", Universidad de Oviedo-CSIC, E-33071 Oviedo, Spain, and Departamento de Química Física y Analítica, Universidad de Oviedo, E-33071 Oviedo, Spain

Received June 30, 2004

The reaction of the cluster complex $[Ru_3(\mu\text{-H})(\mu_3\text{-}\eta^2\text{-apyr})(CO)_9]$ (**1**; Hapyr = 2-aminopyrimidine) with 1,6-diphenoxy-2,4-hexadiyne in refluxing THF gives the trinuclear derivative $[Ru_3(\mu_3\text{-}\eta^2\text{-apyr})(\mu\text{-}\eta^3\text{-PhOCH}_2\text{CH=CC}\equiv\text{CCH}_2\text{OPh})(\mu\text{-CO})_2(CO)_6]$ (**2**), which contains an edge-bridging ynenyl ligand. Heating **2** in refluxing toluene leads to an equilibrium mixture of compounds **2** and $[Ru_3(\mu_3\text{-}\eta^2\text{-apyr})(\mu_3\text{-}\eta^3\text{-PhOCH}_2\text{CH=CC}\equiv\text{CCH}_2\text{OPh})(CO)_8]$ (**3**), in which the ynenyl ligand is in a face-capping position. A mechanistic proposal that accounts for the interconversion of **2** and **3** has been obtained from DFT calculations, which have also revealed that isomer **2** is slightly more stable than **3** (3.5 kcal/mol). The bonding of the ynenyl ligands of **2** and **3** to their corresponding triruthenium frameworks has been studied by MO calculations.

Introduction

Diynes have attracted the attention of organometallic cluster chemists[1−9] because they are more reactive and generally lead to a richer, though more complicated, derivative chemistry than monoalkynes.[10]

Previous studies have shown that amidopyridine-bridged hydridotriruthenium carbonyl complexes[11,12] are ideal candidates for the activation of alkynes, rendering alkenyl derivatives of the type $[Ru_3(\mu_3\text{-}\eta^2\text{-apy})(\mu\text{-}\eta^2\text{-alkenyl})(\mu\text{-CO})_2(CO)_6]$ (apy = 2-amidopyridine-type ligand).[12,13] The face-capping apy ligands help maintain the cluster integrity while still providing reaction pathways of low activation energy.[14]

The natural evolution of these investigations led us to study the reactivity of apy-bridged hydridotriruthenium complexes with diynes. In this field, we have already reported that the complex $[Ru_3(\mu\text{-H})(\mu_3\text{-}\eta^2\text{-ampy})(CO)_9]$ (Hampy = 2-amino-6-methylpyridine) reacts with diphenylbutadiyne,[9] 1,6-diphenoxy-2,4-hexadiyne,[9] and 2,4-hexadiyne[15] to give edge-bridging ynenyl

* To whom correspondence should be addressed. E-mail: jac@fq.uniovi.es. Fax: +34-985103446.
† Departamento de Química Orgánica e Inorgánica.
‡ Departamento de Química Física y Analítica.

(1) (a) Corrigan, J. F.; Doherty, S.; Taylor, N. J.; Carty, A. J. *Organometallics* **1992**, *11*, 3160. (b) Corrigan, J. F.; Doherty, S.; Taylor, N. J.; Carty, A. J. *J. Chem. Soc., Chem. Commun.* **1991**, 1511. (c) Corrigan, J. F.; Doherty, S.; Taylor, N. J.; Carty, A. J. *Organometallics* **1993**, *12*, 1365.

(2) (a)Adams, R. D.; Qu, B. *Organometallics* **2000**, *19*, 2411. (b) Adams, R. D.; Qu, B. *Organometallics* **2000**, *19*, 4090. (c) Adams, R. D.; Qu, B. *J. Organomet. Chem.* **2001**, *619*, 271. (d) Adams, R. D.; Qu, B. *J. Organomet. Chem.* **2001**, *620*, 303.

(3) (a) Bruce, M. I.; Low, P. J.; Werth, A.; Skelton, B. W.; White, A. H. *J. Chem. Soc., Dalton Trans.* **1996**, 1551. (b) Bruce, M. I.; Zaitseva, N. N.; Skelton, B. W.; White, A. H. *Inorg. Chim. Acta* **1996**, *250*, 129. (c) Bruce, M. I.; Zaitseva, N. N.; Skelton, B. W.; White, A. H. *J. Organomet. Chem.* **1997**, *536*−*537*, 93. (d) Adams, C. J.; Bruce, M. I.; Skelton, B. W.; White, A. H. *J. Organomet. Chem.* **1999**, *589*, 213. (e) Bruce, M. I.; Zaitseva, N. N.; Skelton, B. W.; White, A. H. *Russ. Chem. Bull.* **1998**, *47*, 983. (f) Bruce, M. I.; Zaitseva, N. N.; Skelton, B. W.; White, A. H. *Aust. J. Chem.* **1998**, *51*, 165. (g) Bruce, M. I.; Skelton, B. W.; White, A. H.; Zaitseva, N. N. *J. Organomet. Chem.* **1998**, *558*, 197. (h) Bruce, M. I.; Skelton, B. W.; White, A. H.; Zaitseva, N. N. *Inorg. Chem. Commun.* **1998**, *1*, 134. (i) Adams, C. J.; Bruce, M. I.; Skelton, B. W.; White, A. H. *J. Chem. Soc., Dalton Trans.* **1999**, 1283. (j) Bruce, M. I.; Zaitseva, N. N.; Skelton, B. W.; White, A. H. *Dalton* **2002**, 1678. (k) Bruce, M. I.; Skelton, B. W.; White, A. H.; Zaitseva, N. N. *J. Organomet. Chem.* **2002**, *650*, 188.

(4) (a) Clarke, L. P.; Davies, J. E.; Raithby, P. R.; Rennie, M. A.; Shields, G. P.; Sparr, E. *J. Organomet. Chem.* **2000**, *609*, 169. (b) Lau, C. S. W.; Wong, W. T. *J. Chem. Soc., Dalton Trans.* **1999**, 2511.

(5) (a) Tunik, S. P.; Grachova, E. V.; Denisov, V. R.; Starova, G. L.; Nikol'skii, A. B.; Dolgushin, F. M.; Yanovsky, A. I.; Struchkov, Y. T. *J. Organomet. Chem.* **1997**, *536*−*537*, 339. (b) Karpov, M. G.; Tunik, S. P.; Denisov, V. R.; Starova, G. L.; Nikol'skii, A. B.; Dolgushin, F. M.; Yanovsky, A. I.; Struchkov, Y. T. *J. Organomet. Chem.* **1995**, *485*, 219. (c) Tunik, S. P.; Khripun, V. D.; Balova, I. A.; Nordlander, E.; Raithby, P. R. *Organometallics* **2001**, *20*, 3854.

(6) Cabeza, J. A.; Grepioni, F.; Moreno, M.; Riera, V. *Organometallics* **2000**, *19*, 5424.

(7) Unpublished results cited in: (a) Lavigne, G.; Bonneval, B. In *Catalysis by Di- and Polynuclear Metal Cluster Complexes*; Adams, R. D., Cotton. F. A., Eds.; Wiley-VCH: New York, 1998; p 39. (b) Lavigne, G. *Eur. J. Inorg. Chem.* **1999**, 917. (c) Nombel, P. Ph.D. Thesis, Université Paul Sabatier, Toulouse, France, 1996.

(8) Cabeza, J. A.; Moreno, M.; Riera, V.; Rosales, M. J. *Inorg. Chem. Commun.* **2001**, *4*, 57.

(9) Cabeza, J. A.; del Río, I.; García-Granda, S.; Lavigne, G.; Lugan, N.; Moreno, M.; Nombel, P.; Pérez-Priede, M.; Riera, V.; Rodríguez, A.; Suárez, M.; van der Maelen, J. F. *Chem. Eur. J.* **2001**, *7*, 2370.

(10) For a recent review on the reactivity of conjugated diynes with metal complexes, see: Low, P. J.; Bruce, M. I. *Adv. Organomet. Chem.* **2002**, *48*, 72.

(11) (a) Cabeza, J. A.; Oro, L. A.; Tiripicchio, A.; Tiripicchio-Camellini, M. *J. Chem. Soc., Dalton Trans.* **1988**, 1437. (b) Andreu, P. L.; Cabeza, J. A.; Riera, V.; Jeannin, Y.; Miguel, D. *J. Chem. Soc., Dalton Trans.* **1990**, 2201. (c) Lugan, N.; Laurent, F.; Lavigne, G.; Newcomb, T. P.; Liimata, E. W.; Bonnet, J. J. *Organometallics* **1992**, *11*, 1351.

(12) Lugan, N.; Laurent, F.; Lavigne, G.; Newcomb, T. P.; Liimata, E. W.; Bonnet, J. J. *J. Am. Chem. Soc.* **1990**, *112*, 8607.

(13) (a) Cabeza, J. A.; Fernández-Colinas, J. M.; Llamazares, A.; Riera, V. *J. Mol. Catal.* **1992**, *71*, L7. (b) Cabeza, J. A.; Fernández-Colinas, J. M.; Llamazares, A.; Riera, V.; García-Granda, S.; van der Maelen, J. F. *Organometallics* **1994**, *13*, 4352 and references therein.

(14) Shen, J. K.; Basolo, F.; Nombel, P.; Lugan, N.; Lavigne, G. *Inorg. Chem.* **1996**, *35*, 755.

10.1021/om049524o CCC: $27.50
Publication on Web 10/23/2004

Scheme 1

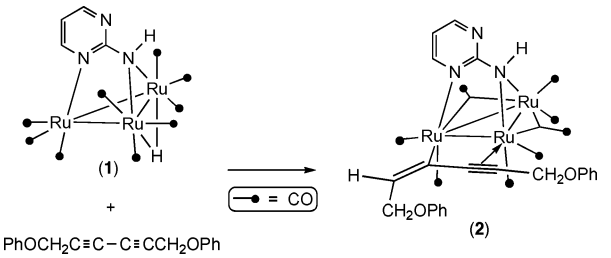

Scheme 2

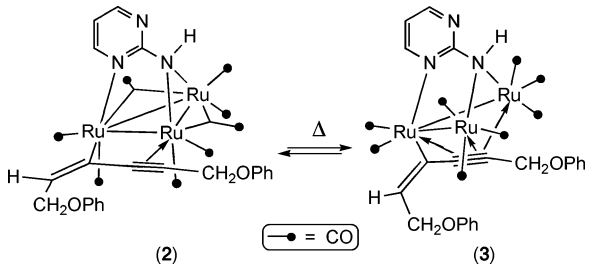

derivatives which are prone to react further with alkynes and diynes to give interesting coupling products, such as η^5-cyclopentadienyl,[9] η^5-ruthenacyclopentadienyl,[9] and diynedienyl[15] derivatives. The complex $[Ru_3(\mu\text{-H})(\mu_3\text{-}\eta^2\text{-apyr})(CO)_9]$ (**1**; Hapyr = 2-aminopyrimidine) also reacts with 2,4-hexadiyne[16] and diphenylbutadiyne[17] to give ynenyl derivatives that are capable of incorporating two additional diyne molecules, rendering products that contain large unsaturated hydrocarbon ligands. For example, we have recently described the formation of a highly functionalized azulene ligand by metal cluster mediated coupling of three conjugated diynes.[17]

We now report (a) that the study of the reactivity of the 2-amidopyrimidine-bridged complex **1** with 1,6-diphenoxy-2,4-hexadiyne has led us to observe a change of the coordination mode of an ynenyl ligand from edge bridging to face capping on a triruthenium cluster, (b) that a possible mechanism for such an isomerization process has been envisaged with the help of DFT calculations, and (c) that for both coordination modes, simple MO calculations have shed light on the nature of the orbital interactions between the ynenyl ligand and the corresponding triruthenium fragments.

Results and Discussion

Synthesis and Structural Characterization of 2 and 3. The treatment of compound **1** with 1.5 equiv of 1,6-diphenoxy-2,4-hexadiyne (refluxing THF, 30 min) allowed the isolation of the trinuclear derivative $[Ru_3(\mu_3\text{-}\eta^2\text{-apyr})(\mu\text{-}\eta^3\text{-PhOCH}_2\text{CH=CC}\equiv\text{CCH}_2\text{OPh})(\mu\text{-CO})_2(CO)_6]$ (**2**) in 72% yield (Scheme 1).

Compound **2** was characterized by analytical and spectroscopic techniques. Its trinuclear nature was indicated by its microanalysis and mass spectrum, which shows the molecular ion. Its IR spectrum shows the presence of two bridging CO ligands. The ^{1}H NMR spectrum also confirms the transfer of a hydrogen atom (the hydride ligand of **1**) to the original diyne to give an ynenyl ligand. The multiplicity of the signal of this hydrogen atom (triplet, J = 6.7 Hz) indicates that it is adjacent to a methylene group. The structure depicted for compound **2** in Scheme 1, which shows an edge-bridging three-electron-donor 1,6-diphenoxyhex-2-yn-4-en-4-yl ligand, is also supported by the similarity of its spectroscopic data with those reported for the compounds $[Ru_3(\mu_3\text{-}\eta^2\text{-ampy})(\mu\text{-}\eta^3\text{-RCH=CC}\equiv\text{CR})(\mu\text{-CO})_2(CO)_6]$ (R = Ph, CH_2OPh), the structures of which have been determined by X-ray diffraction methods.[9] In that article, a mechanistic proposal accounting for the formation of compounds similar to **2** from hydrido trinuclear clusters and conjugated diynes is also reported.[9]

Apart from the compounds mentioned in the Introduction, only a few more ynenyl derivatives have so far been reported as products of reactions of ruthenium carbonyl clusters with diynes. They are the complexes $[Ru_2(\mu\text{-N=CPh}_2)(\mu\text{-}\eta^2\text{-CH}_2\text{=CCH}_2\text{C}\equiv\text{CSiMe}_3)(CO)_6]$,[6] $[Ru_3(\mu_3\text{-}\eta^2\text{-pyNMe})(\mu\text{-}\eta^3\text{-PhCH=CC}\equiv\text{CPh})(\mu\text{-CO})_2(CO)_6]$,[7] and $[Ru_4(\mu\text{-}\eta^2\text{-dmpz})(\mu_4\text{-}\eta^4\text{-MeCH=CC}\equiv\text{CMe})(\mu\text{-CO})(CO)_{10}]$ (Hdmpz = 3,5-dimethylpyrazole),[8] which arise from the insertion of conjugated diynes into a metal−hydride bond of trinuclear cluster precursors. An additional ruthenium cluster complex containing an ynenyl ligand has been reported, $[Ru_3\{\mu\text{-NS(O)MePh}\}(\mu_3\text{-}\eta^3\text{-PhCH=CC}\equiv\text{CPh})(CO)_9]$.[18] As it contains a face-capping ynenyl ligand, additional comments on this cluster complex are given below.

In an attempt to shorten the reaction time for the synthesis of compound **2**, we performed the reaction of complex **1** with 1,6-diphenoxy-2,4-hexadiyne in refluxing toluene. This time, two reaction products were observed: i.e., **2** and a new complex which was subsequently identified as $[Ru_3(\mu_3\text{-}\eta^2\text{-apyr})(\mu_3\text{-}\eta^3\text{-PhOCH}_2\text{CH=CC}\equiv\text{CCH}_2\text{OPh})(CO)_8]$ (**3**). The thermolysis of complex **2** in refluxing toluene for 20 min also led to a ca. 50% mixture of **2** and **3** (^{1}H NMR integration of the crude reaction mixture). Longer reaction times did not change the **2**:**3** ratio but only increased the amount of intractable decomposition products. Heating **3** in refluxing toluene for 20 min also led to a ca. 50% mixture of **2** and **3** (^{1}H NMR integration of the crude reaction mixture). Therefore, both compounds interconvert into each other under these reaction conditions to give ca. 50% of each complex in the equilibrium (Scheme 2).

The molecular structure of compound **3** was determined by X-ray diffraction methods (Figure 1). The ruthenium atoms define an isosceles triangle with an edge, Ru(2)−Ru(3), ca. 0.35 Å longer than the other two. The apyr ligand caps a face of the metal triangle in the same way as that previously found in other 2-amidopyridine-capped trinuclear clusters.[9,11−15] The ynenyl ligand caps the opposite face of the metal triangle through only three carbon atoms, C(20), C(21), and C(22), in such a way that the alkenyl fragment is σ-bonded to Ru(1) through C(22), and the C≡C fragment is attached to the three metal atoms in a perpendicular fashion:[19] i.e., the C(20)−C(21) vector is perpendicular to the Ru(2)−Ru(3) vector. The carbon−carbon double bond of the alkenyl fragment, C(22)−C(23), is not coordinated. All

(15) Cabeza, J. A.; del Río, I.; García-Granda, S.; Moreno, M.; Riera, V. *Organometallics* **2001**, *20*, 4993.
(16) Cabeza, J. A.; del Río, I.; Moreno, M.; García-Granda, S.; Pérez-Priede, M.; Riera, V. *Eur. J. Inorg. Chem.* **2002**, 3204.
(17) Cabeza, J. A.; del Río, I.; García-Granda, S.; Martínez-Méndez, L.; Moreno, M.; Riera, V. *Organometallics* **2003**, *22*, 1164.
(18) Ferrand, V.; Gambs, C.; Derrien, N.; Bolm, C.; Stoeckli-Evans, H.; Süss-Fink, G. *J. Organomet. Chem.* **1997**, *549*, 275.

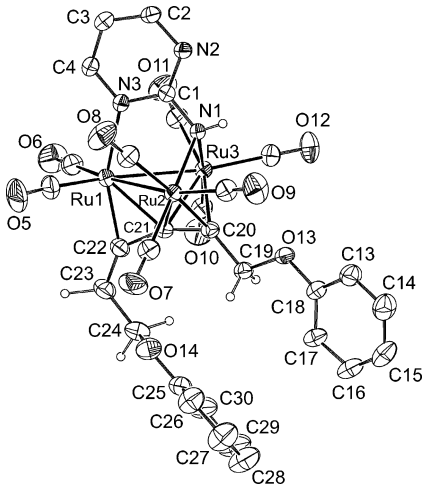

Figure 1. Molecular structure of compound **3**. Selected interatomic distances (Å): Ru(1)−Ru(2) = 2.848(2), Ru(1)−Ru(3) = 2.881(2), Ru(2)−Ru(3) = 3.218(2), Ru(1)−N(3) = 2.221(3), Ru(1)−C(21) = 2.171(4), Ru(1)−C(22) = 2.033(4), Ru(2)−N(1) = 2.180(3), Ru(2)−C(20) = 2.179(3), Ru(2)−C(21) = 2.283(4), Ru(3)−N(1) = 2.177(3), Ru(3)−C(20) = 2.207(3), Ru(3)−C(21) = 2.242(4), C(19)−C(20) = 1.480(5), C(20)−C(21) = 1.350(5), C(21)−C(22) = 1.416(5), C(22)−C(23) = 1.325(5), C(23)−C(24) = 1.496(7). Selected interatomic angles (deg): C(19)−C(20)−C(21) = 129.2(3), C(20)−C(21)−C(22) = 158.2(3), C(21)−C(22)−C(23) = 135.6(4), C(22)−C(23)−C(24) = 121.9(4).

six carbon atoms of the hexynenyl moiety and the atoms of the apyr ligand are coplanar, and this plane is perpendicular to the metal triangle. The cluster shell is completed with eight terminal carbonyl ligands. Therefore, the cluster can be considered as a 50-electron species with only two Ru−Ru bonds, the ynenyl ligand behaving as a 5-electron donor.

The ^{1}H NMR spectrum of **3** shows that both H atoms of each methylene group are equivalent. Therefore, in solution, the complex displays C_s symmetry, probably due to free rotation about the C(23)−C(24) and C(19)−C(20) single bonds. Accordingly, the alkenyl proton is observed as a triplet, due to coupling with the protons of the adjacent methylene group.

As noted above, the complex [Ru_3{μ-NS(O)MePh}(μ_3-η^3-PhCH=CC≡CPh)$(CO)_9$] is, to our knowledge, the only precedent in ruthenium chemistry of a cluster complex containing an ynenyl ligand coordinated in a way similar to that found in **3**. Curiously, the butynenyl ligand of [Ru_3{μ-NS(O)MePh}(μ_3-η^3-PhCH=CC≡CPh)-$(CO)_9$] does not arise from a diyne but from an alkynyl−vinylidene coupling and the N-donor sulfoximido ligand is not face capping but edge bridging.[18] In the related complex [Ru_3{μ_3-NS(O)MePh}(μ_3-η^3-PhCH=C=C=CPh)-(μ-CO)$(CO)_7$], the bridging hydrocarbyl ligand is best described as a buta-1,2,3-trien-1-yl fragment, rather than as a but-1-yn-3-en-4-yl fragment.[18] A few triosmium carbonyl clusters containing butynenyl ligands that asymmetrically cap a face of the metal triangle have been recently reported. In these cases, the butynenyl ligands are derived from bis(ferrocenyl)butadiyne.[2b]

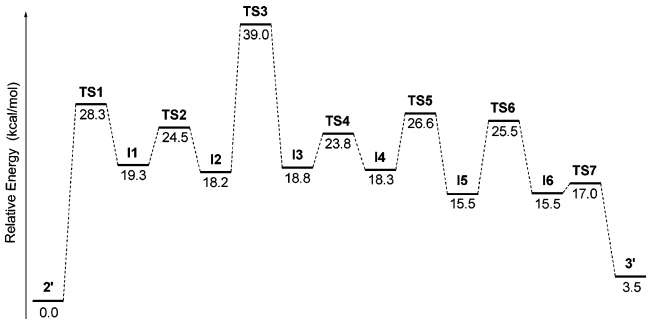

Figure 2. Energy profile for the interconversion of **2′** and **3′**.

Mechanism of Interconversion of Complexes 2 and 3. As noted above, complexes **2** and **3** interconvert in toluene at reflux temperature. Since the interconversion of edge-bridging and face-capping ynenyl ligands on a trimetal core had no precedents, we decided to undertake a theoretical mechanistic study of this process by DFT calculations.

To simplify the calculations without losing chemical information, compounds **2** and **3** were modeled by changing their 1,6-diphenoxyhex-2-yn-4-en-4-yl ligand to a pent-2-yn-4-en-4-yl ligand. Hereafter, these model compounds will be named **2′** and **3′**.

We first optimized the structures of the model complexes **2′** and **3′**. The input data were based on the X-ray structural data of the complexes [Ru_3(μ_3-η^2-ampy)(μ-η^3-PhCH=CC≡CPh)(μ-CO)$_2$$(CO)_6$][9] and **3**, which were conveniently modified by replacing some atoms in order to transform them into **2′** and **3′**, respectively. The calculated structures of **2′** and **3′** are in reasonable agreement with the experimental X-ray structures of [Ru_3(μ_3-η^2-ampy)(μ-η^3-PhCH=CC≡CPh)(μ-CO)$_2$$(CO)_6$][9] and **3**, the greatest divergences corresponding to the Ru−Ru distances, which are 0.06−0.10 Å longer in the model compounds than in the real complexes. The overestimation of the optimized Ru−Ru distances is expected at the GGA level. As far as energy is concerned, the models **2′** and **3′** differ by only 3.5 kcal/mol, the former being more stable. This explains why, once the interconversion equilibrium was reached, **2** and **3** were obtained as ca. 50% mixtures.

The search for transition states and intermediate species on the potential energy surface was very tedious and time-consuming. This was due to the large number of atoms involved (including three transition-metal atoms) and the complicated nature of the resulting mechanism, for which seven transition states (hereafter labeled as **TS1**−**TS7**) and six intermediate species (hereafter labeled as **I1**−**I6**) were found to connect **2′** and **3′** (Figures 2 and 3, Table 1).

Transition state **TS1** is 28.3 kcal/mol less stable than **2′** and 9.0 kcal/mol less stable than **I1**. In the transformation of **2′** into **I1**, the lengthening of the Ru(1)−Ru(3) distance (from 3.031 Å in **2′** to 3.777 Å in **TS1** and 4.529 Å in **I1**) is accompanied by the conversion of the two bridging CO ligands into terminal ones, the folding of the ynenyl fragment (from 179.0° in **2′** to 144.0° in **I1**), and its slippage from its initial situation to a new one that involves the lengthening of the C(21)−Ru(1)

(19) Complexes containing alkyne ligands coordinated to three ruthenium atoms in a perpendicular fashion are scarce. See, for example: (a) Ferrand, V.; Merzweiler, K.; Rheinwald, G.; Stoeckli-Evans, H.; Süss-Fink, G. *J. Organomet. Chem.* **1997**, *549*, 263. (b) Rivomanana, S.; Lavigne, G.; Lugan, N.; Bonnet, J. J. *Inorg. Chem.* **1991**, *30*, 4110. (c) Rivomanana, S.; Mongin, C.; Lavigne, G. *Organometallics* **1996**, *15*, 1195.

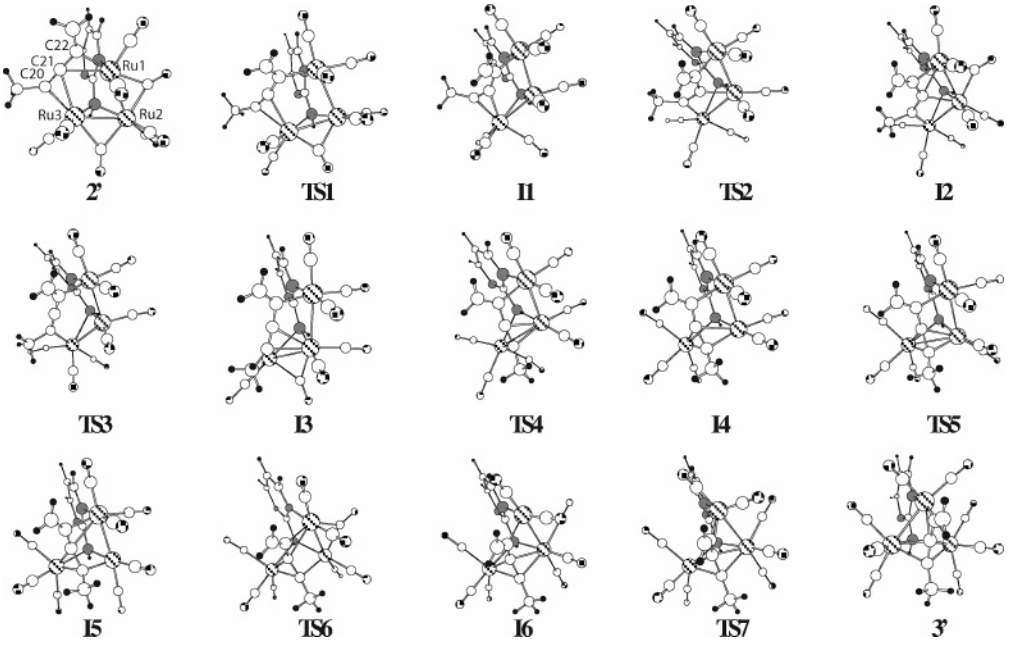

Figure 3. DFT-calculated structures of the intermediates (**I**) and transition states (**TS**) involved in the interconversion of **2′** and **3′**. In all structures, the apyr ligand is behind the metallic triangle.

Table 1. Structural Parameters for the Intermediates (I) and Transition States (TS) Involved in the Interconversion of Compounds 2′ and 3′

	2′	**TS1**	**I1**	**TS2**	**I2**	**TS3**	**I3**	**TS4**	**I4**	**TS5**	**I5**	**TS6**	**I6**	**TS7**	**3′**
							Relative Energy (kcal/mol)								
	0.00	28.28	19.26	24.47	18.23	39.02	18.82	23.76	18.28	26.61	15.46	25.46	15.47	16.95	3.49
							Distances (Å)								
Ru(1)−Ru(2)	2.849	2.898	2.721	2.772	2.784	2.780	2.941	2.854	2.837	2.880	2.857	2.934	2.842	2.862	2.950
Ru(1)−Ru(3)	3.031	3.777	4.529	4.639	4.585	4.594	4.795	4.647	4.376	4.273	3.992	4.080	4.121	3.773	2.950
Ru(2)−Ru(3)	2.753	2.762	2.731	2.781	2.745	2.657	2.794	2.834	3.112	2.883	3.161	3.149	3.307	3.300	3.283
C(20)−Ru(2)	4.593	4.510	3.547	3.008	2.835	3.131	2.363	2.330	2.265	2.081	2.093	2.331	2.274	2.254	2.231
C(20)−Ru(3)	2.184	2.323	2.141	2.036	2.074	2.271	2.382	2.369	2.200	2.210	2.143	2.133	2.144	2.144	2.232
C(21)−Ru(3)	2.638	2.352	2.326	2.681	3.005	3.230	3.213	2.783	2.172	2.177	2.125	2.138	2.147	2.176	2.336
C(21)−Ru(2)	4.462	3.977	2.626	2.117	2.346	3.057	2.246	2.502	2.550	2.289	2.703	2.807	2.429	2.379	2.337
C(21)−Ru(1)	2.588	2.986	2.966	2.532	2.232	2.859	2.723	2.830	2.811	2.611	2.412	2.487	2.630	2.440	2.232
C(22)−Ru(1)	2.112	2.150	2.136	2.139	2.136	2.224	2.120	2.127	2.137	2.099	2.239	2.094	2.066	2.050	2.043
N(3)−Ru(1)	2.206	2.234	2.282	2.266	2.245	2.227	2.235	2.236	2.253	2.251	2.232	2.216	2.238	2.306	2.301
N(1)−Ru(2)	2.206	2.153	2.144	2.165	2.154	2.133	2.183	2.154	2.152	2.152	2.179	2.165	2.186	2.206	2.228
N(1)−Ru(3)	2.226	2.238	2.310	2.295	2.224	2.323	2.246	2.250	2.287	2.321	2.315	2.314	2.294	2.277	2.228
							Angles (deg)								
C(20)−C(21)−C(22)	179.0	168.5	144.0	123.9	128.7	179.7	173.1	168.5	148.0	147.1	146.6	145.4	149.5	147.2	160.6
C(21)−C(22)−C(23)	132.6	120.4	121.3	136.6	148.3	130.5	126.3	123.3	126.5	131.3	147.6	138.0	133.4	136.5	136.2
Ru(1)−Ru(2)−Ru(3)	65.5	83.7	112.3	113.4	112.1	115.3	113.4	109.4	94.6	95.7	82.9	84.2	83.8	75.1	56.2
C(20)−Ru(3)−Ru(2)−Ru(1)	27.4	26.8	−17.8	−33.3	−39.4	−43.2	−71.3	−78.2	−86.4	−87.0	−82.9	−76.0	−100.7	−105.9	−111.9

distance (from 2.588 Å in **2′** to 2.966 Å in **I1**) and the approximation of C(21) to Ru(2) (4.462 Å in **2′** and 2.626 Å in **I1**).

From **I1** to **I2**, the C(21) atom continues its approach to Ru(2) (2.346 Å in **I2**) at the same time that it moves away from Ru(3) (3.005 Å in **I2**) and again gets close to Ru(1) (2.232 Å in **I2**). These movement of the ynenyl fragment implies an important bending of the C(20)−C(21)−C(22) angle (128.7° in **I2**). The three carbonyl ligands on Ru(3) undergo a tripodal rotation that is accompanied by a movement of a CO ligand from a terminal position on Ru(1) to a bridging position between Ru(1) and Ru(2).

The most important structural change from **I2** to **I3** is that C(20), which is attached to Ru(3) in **I2**, spans the Ru(2)−Ru(3) edge in **I3**. This situation will be maintained all the way to **3′**. To reach this situation, the C(21) carbon atom is released from Ru(2) to give a nearly linear ynenyl fragment (**TS3**) that subsequently bends toward Ru(2), allowing the coordination of C(20) and C(21) to this metal atom (**I3**). One of the CO ligands attached to Ru(3) in **I2** moves from a terminal to a bridging position between Ru(2) and Ru(3), and the bridging CO ligand of **I2** moves to a terminal position on the Ru(1) atom of **I3**. The high coordinative unsaturation of **TS3** (only two Ru−Ru bonds and only two $Ru-C_{ynenyl}$ bonds) accounts for the high energy of this transition state (39.0 kcal/mol above **2′**).

From **I3** to **I4**, the shortening of the Ru(1)−Ru(3) distance (from 4.795 Å in **I3** to 4.376 Å in **I4**) induces the coordination of C(21) to Ru(3). This is accompanied by a lengthening of the Ru(2)−Ru(3) distance to 3.112 Å and by a movement of the bridging CO ligand of **I3** to a terminal position on the Ru(3) atom of **I4**.

From **I4** to **I5**, the Ru(1) and Ru(3) atoms get closer (3.992 Å in **I5**). This provokes the approach of C(21) to Ru(1) (2.412 Å in **I5**) and the lengthening of the C(21)−Ru(2) distance (from 2.550 Å in **I4** to 2.703 Å in **I5**).

From **I5** to **I6**, the ynenyl ligand moves toward its final position in **3′** and the Ru(2)−Ru(3) distance lengthens (3.307 Å in **I6**). This causes the lengthening of the C(21)−Ru(1) distance (2.630 Å in **I6**) and the shortening of the C(21)−Ru(2) distance (2.429 Å in **I6**). A CO ligand, originally attached to Ru(1), is transferred to Ru(2).

From **I6** to **3′**, the ynenyl ligand moves to its final position and the Ru(1)−Ru(3) edge shortens to a bonding distance (from 4.121 Å to 2.950 Å). This step has a very low activation energy (1.5 kcal/mol) and results in a considerable stabilization of the system, because the coordinative unsaturation of **I6** is eliminated in **3′** (the latter is 12.02 kcal/mol more stable than **I6**).

The activation energy of the whole interconversion process is associated with the energy of the least stable transition state, **TS3**. The relatively high value of this energy, 39.0 kcal/mol above **2′** and 35.5 kcal/mol above **3′**, implies that the interconversion of **2′** and **3′** should take place only at high temperatures. This matches the experimental observation that the interconversion of **2** and **3** takes place in refluxing toluene, but it is not observed in refluxing THF. The low energy of **2′** and **3′** (as compared with those of all intermediate species **I1**−**I6**) and the low energy of the transition states **TS1**, **TS2**, and **TS4**−**TS7** (as compared with that of **TS3**) also explain the fact that no intermediate species have been observed during the interconversion of **2′** and **3′**. All these facts support the proposed mechanism. Although an alternative mechanism involving CO dissociation and reassociation steps (**2** and **3** have the same number of CO ligands) cannot be completely ruled out, we think it would be less likely than the proposed mechanism, because CO would rapidly escape from the reacting solution at the working temperature and this would lead to extensive decomposition.

Orbital Interactions between the Ynenyl Ligands and the Trimetallic Fragments of 2 and 3. A simple fragment molecular orbital (FMO) approach, at the extended Hückel level, allowed us to identify the FMOs that are responsible for the bonding between the ynenyl and triruthenium fragments of **2** and **3**. The characteristics of the bonding between these fragments were elucidated by analyzing the overlaps between their FMOs. Again, the simplified model compounds **2′** and **3′** were used for the calculations.

For **2′**, three interactions between FMOs of the ynenyl fragment and FMOs of the trimetallic fragment account for 91.5% of the bonding between these two fragments (Figure 4). Many other minor interactions are responsible for the remaining 8.5%. The ynenyl fragment behaves as a σ-donor−π-acceptor ligand, the σ-donor component being mainly due to the bonding interactions of the filled FMO11 and FMO13 orbitals of the ynenyl ligand (its LUMO is FMO14, not represented in Figure 4) with the empty FMO71 and FMO70 orbitals, respectively, of the metallic fragment (its LUMO is FMO70). The interaction of the HOMO of the metallic fragment (FMO69) with the empty orbital FMO15 of the ynenyl fragment is the major orbital interaction responsible for the retrodonation of electron density from the metal atoms to the ynenyl ligand (π-acception).

For complex **3′**, Figure 5 represents the four orbital interactions between the FMOs of the ynenyl and the

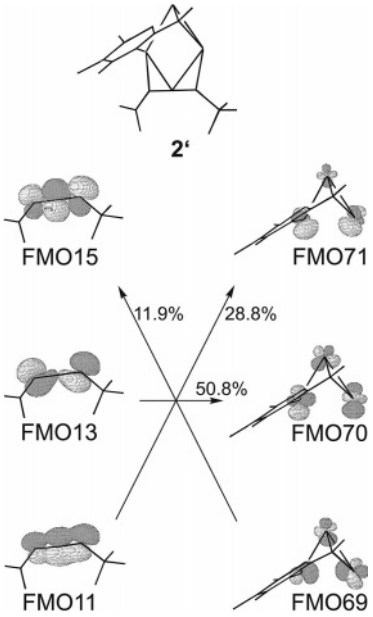

Figure 4. The most important overlaps between orbitals of the ynenyl (left) and triruthenium (right) fragments of **2′**. The arrows connect the overlapping filled (start) and empty (end) orbitals. The percentages represent the contribution of each overlap to the bonding between the two fragments. For clarity, CO ligands have been omitted.

trimetallic fragments that individually account for more than 12% of the bonding. They all represent 71.1% of the bonding between these two fragments. As in **2′**, the ynenyl fragment of **3′** is a σ-donor−π-acceptor ligand, the principal σ-donor contributions being the bonding interactions of the filled FMO11 and FMO13 orbitals of the ynenyl ligand with the empty FMO71 and FMO70 orbitals, respectively, of the metallic fragment, while the most important π-accepting contributions are the interactions of the filled metallic orbitals FMO68 and FMO69 with the empty orbitals FMO14 and FMO15, respectively, of the ynenyl fragment.

An analysis of the individual overlap populations between the carbon atoms C(20), C(21), and C(22) and the three metal atoms of **2′** indicates that, while strong overlaps are observed between C(20) and C(22) with Ru(3) and Ru(1), respectively, the orbitals of C(21) overlap very little with those of Ru(1) and Ru(3). This bonding situation is due to the fact that the interaction of the triple bond of the ynenyl ligand with the Ru(3) metal atom is very asymmetric. In fact, in the DFT-optimized molecule **2′**, the distances that separate C(20) and C(21) from Ru(3) are 2.180 and 2.638 Å, respectively, the latter being very similar to the separation between C(21) and Ru(1), 2.588 Å.

For complex **3′**, an analogous analysis shows that the highest overlap population corresponds to that between C(22) and Ru(1), followed by those of C(20) with Ru(2) and Ru(3). The orbitals of the C(21) carbon atom clearly overlap with those of the three metal atoms, the C(21)−Ru(1) overlap population being slightly greater than those of C(21)−Ru(2) and C(21)−Ru(3). This bonding situation is that expected for a face-capping ynenyl ligand interacting with the three metal atoms through both carbon atoms of its C≡C triple bond (in a perpendicular fashion[19]), being additionally bonded to one metal atom through the carbon atom of its C=C frag-

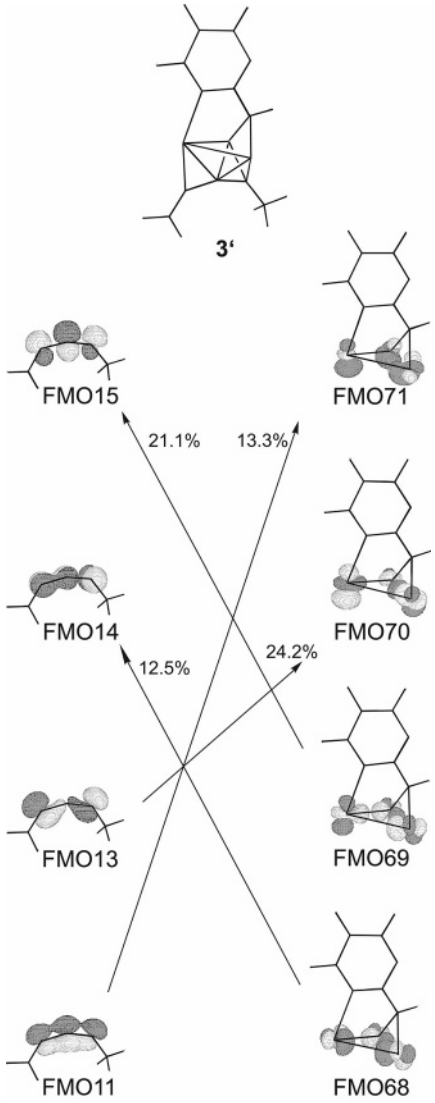

Figure 5. The most important overlaps between orbitals of the ynenyl (left) and triruthenium (right) fragments of **3′**. The arrows connect the overlapping filled (start) and empty (end) orbitals. The percentages represent the contribution of each overlap to the bonding between the two fragments. For clarity, CO ligands have been omitted.

ment that is attached to one of the carbon atoms involved in the C≡C triple bond.

It is interesting to note that, for **2′**, the sum of the overlap populations found between the carbon atoms C(20), C(21), and C(22) with the three metal atoms is ca. 45% smaller than that found for complex **3′**. This is in reasonable agreement with the assignment of the ynenyl ligand as a three-electron donor in complex **2′** and as a five-electron donor in complex **3′**.

Concluding Remarks

The present work describes the synthesis of two isomeric triruthenium carbonyl complexes that contain edge-bridging (**2**) and face-capping (**3**) ynenyl ligands. It has been shown that these two complexes interconvert at high temperature (refluxing toluene). A plausible mechanism for this interconversion has been elucidated with the help of DFT calculations. The fragment molecular orbitals that are responsible for the bonding between the ynenyl and the triruthenium fragments of both the edge-bridged and face-capped ynenyl complexes have been identified. A study of the overlaps between these orbitals has shown that the ynenyl fragment behaves as a σ-donor−π-acceptor ligand in both complexes.

Experimental Section

General Data. Solvents were dried over sodium diphenyl ketyl (THF, hydrocarbons) or CaH_2 (dichloromethane) and distilled under nitrogen prior to use. The reactions were carried out under nitrogen, using Schlenk and vacuum line techniques, and were routinely monitored by solution IR spectroscopy (carbonyl stretching region) and spot TLC. Compound **1** was prepared as described previously.[16] IR spectra were recorded in solution on a Perkin-Elmer Paragon 1000 FT spectrophotometer. NMR spectra were run at room temperature on a Bruker DPX-300 instrument, using the dichloromethane solvent resonance (δ 5.33) as internal standard. Microanalyses were obtained from the University of Oviedo Analytical Service. Positive FAB-MS measurements were obtained from the University of Santiago de Compostela Mass Spectrometric Service; data given refer to the most abundant molecular ion isotopomer.

[$Ru_3(\mu_3$-η^2-apyr)(μ-η^3-PhOCH$_2$CH=CC≡CCH$_2$OPh)(μ-CO)$_2$(CO)$_6$] (2). 1,6-Diphenoxy-2,4-hexadiyne (170 mg, 0.648 mmol) was added to a solution of compound **1** (275 mg, 0.423 mmol) in THF (20 mL). The solution was heated at reflux temperature until the IR spectrum showed the complete disappearance of the starting complex (ca. 30 min, IR monitoring). The color changed from yellow to dark red. The solvent was removed under reduced pressure, the residue was dissolved in 2 mL of dichloromethane, and the resulting solution was placed on a column of neutral alumina (2 × 5 cm, activity IV) packed in hexane. After the column was washed with hexane, hexane−dichloromethane (1:1) eluted a yellow band, which afforded compound **2** upon solvent removal (270 mg, 72%). Anal. Calcd for $C_{30}H_{19}N_3O_{10}Ru_3$ (M_r = 884.69): C, 40.72; H, 2.16; N, 4.74. Found: C, 40.73; H, 2.07; N, 4.68. FAB MS: *m/z* 886 [M^+]. IR (THF): ν_{CO} 2069 (s), 2031 (vs), 2001 (s), 1977 (sh), 1878 (w), 1829 (m) cm^{-1}. ^{1}H NMR ($CDCl_3$): δ 7.95 (dd, J = 4.8, 2.6 Hz, 1 H, H_{apyr}), 7.81 (dd, J = 5.7, 2.6 Hz, 1 H, H_{apyr}), 7.2−6.9 (m, 8 H, Ph), 6.90 (dd, J = 6.7, 2.3 Hz, 1 H, C*H*H), 6.82 (d, J = 8.6 Hz, 1 H, Ph), 6.68 (t, J = 6.7 Hz, 1 H, =CH), 6.54 (d, J = 8.5 Hz, 1 H, Ph), 6.35 (dd, J = 5.7, 4.8 Hz, 1 H, H_{apyr}), 5.80 (d, J = 15.9 Hz, 1 H, C*H*H), 5.38 (d, J = 15.9 Hz, 1 H, C*H*H), 4.99 (dd, J = 6.7, 2.3 Hz, 1 H, C*H*H), 2.73 (s, br, 1H, NH_{apyr}).

[$Ru_3(\mu_3$-η^2-apyr)(μ_3-η^3-PhOCH$_2$CH=CC≡CCH$_2$OPh)-(CO)$_8$] (3). A solution of compound **2** (150 mg, 0.169 mmol) in toluene (20 mL) was heated at reflux temperature for 20 min. The color changed from yellow to brown. The solvent was partially removed under reduced pressure, and the resulting solution (ca. 1 mL) was placed on a column of neutral alumina (2 × 8 cm, activity IV) packed in hexane. After the column was washed with hexane, a broad yellow band was eluted with hexane−dichloromethane (1:1). The head of this band contained pure complex **3**, which was isolated as a yellow solid after solvent removal (19 mg, 13%). The remaining portion of the band contained a mixture of compounds **2** and **3**, for which no subsequent separation was attempted. Anal. Calcd for $C_{30}H_{19}N_3O_{10}Ru_3$ (M_r = 884.69): C, 40.72; H, 2.16; N, 4.74. Found: C, 40.80; H, 2.23; N, 4.62. FAB MS: *m/z* 886 [M^+]. IR (CH_2Cl_2): ν_{CO} 2085 (w), 2068 (vs), 2016 (s), 1995 (sh), 1944 (m) cm^{-1}. ^{1}H NMR ($CDCl_3$): δ 8.73 (dd, J = 5.3, 2.3 Hz, 1 H, H_{apyr}), 8.02 (dd, J = 4.8, 2.3 Hz, 1 H, H_{apyr}), 7.9−6.5 (m, 12 H), 5.67 (t, J = 6.5 Hz, 1 H, =CH), 5.21 (s, 2 H, CH_2), 4.42 (d, J = 6.5 Hz, 2 H, CH_2).

X-ray Structure of 3. The crystal was selected from a batch obtained by slow diffusion of a layer of pentane into a solution

of **3** in toluene. Details of crystal and refinement data are given in ref 20. X-ray diffraction data were collected on a Nonius CAD-4 diffractometer, using graphite-monochromated Mo Kα radiation and the $\omega-2\theta$ scan technique. An empirical absorption correction was applied using DIFABS,[21] with transmission factors in the range 0.762−0.338. The structure was solved by Patterson interpretation using the program DIRDIF-96.[22] Isotropic and full-matrix anisotropic least-squares refinements were carried out using SHELXL-97.[23] All non H-atoms were refined anisotropically. All H atoms were located on Fourier difference maps and were refined freely with isotropic thermal parameters. The molecular plot was made with PLATON.[24] All operations were performed within the WinGX program system.[25] The CCDC deposition number is 249358.

Computational Details. Density functional theory calculations were performed using Becke's three-parameter hybrid exchange-correlation functional (DFT/Hartree−Fock)[26] containing the nonlocal gradient correction of Lee, Yang, and Parr (B3LYP).[27] The basis set used for Ru was the LanL2DZ of Hay and Wadt with the associated double-ζ valence basis functions.[28] The standard 6-31G basis set, with addition of (d,p)-polarization, was used for the remaining atoms. Transition states were found using the QST2/QST3 method. All stationary points were confirmed as minima or as transition states by calculation of analytical frequencies. To verify that the transition states found were correct saddle points connecting the proposed minima, the structure of each transition state was first distorted forward and back along the unique imaginary eigenvector and then it was allowed to relax to the corresponding minimum (reactant or product) in subsequent structure optimizations. All these calculations were performed using the GAUSSIAN98 software package.[29]

EHMO calculations and orbital diagrams were performed with the CACAO software package.[30]

Acknowledgment. This work has been supported by the MCYT grants BQU2002-2623 (to J.A.C.) and BQU2003-5093 to (S.G.-G.). M.M. thanks the MECD for a predoctoral fellowship (FPI program).

Supporting Information Available: Tables giving crystallographic data for **3** and atomic coordinates for the DFT-calculated structures of **2′**, **3′,** and all the intermediates and transition states involved in the interconversion of **2′** and **3′**. This material is available free of charge via the Internet at http://pubs.acs.org.

OM049524O

(20) Crystal and selected refinement data for **3**: $C_{30}H_{19}N_3O_{10}Ru_3$; fw = 884.69; crystal size 0.40 × 0.33 × 0.33 mm; crystal system triclinic; space group $P\bar{1}$; a = 9.209(5) Å; b = 11.477(7) Å; c = 16.107(2) Å; α = 96.44(4)°; β = 98.92(4)°; γ = 99.33(7); V = 1643(1) Å^3; Z = 2; ρ_{calcd} = 1.788 g/cm^3; λ = 0.710 73 Å; μ = 1.419 mm^{-1}; $F(000)$ = 864; index range $0 \le h \le 11$, $-14 \le k \le 13$, $-19 \le l \le 19$; θ range 1.82−25.97°; T = 293(2) K; collected reflections 6838; unique reflections 6421; R_{int} = 0.0252; reflections with $I < 2\sigma(I)$ 5480; variables 491; weighting scheme $w = 1/[\sigma^2F_o^2 + (0.0453P)^2 + 1.5071P]$, $P = (F_o^2 + 2F_c^2)/3$; GOF = 1.063; final $R1_{2\sigma(I)}$ = 0.0292; final $wR2_{all\ data}$ = 0.0827; largest difference peak and hole 0.754 and −0.783 e/Å^3.

(21) Walker, N.; Stuart, D. *Acta Crystallogr.* **1983**, *A39*, 158.

(22) (a) Beurskens, P. T.; Beurskens, G.; Bosman, W. P.; de Gelder, R.; García-Granda, S.; Gould, R. O.; Israël, R.; Smits, J. M. M. *The DIRDIF-96 Program System*; Crystallography Laboratory, University of Nijmegen, Nijmegen, The Netherlands, 1996.

(23) Sheldrick, G. M. *SHELXL97, version 97-2*; University of Göttingen, Göttingen, Germany, 1997.

(24) Spek, A. L. *PLATON: A Multipurpose Crystallograhic Tool*; University of Utrecht, Utrecht, The Netherlands, 2003.

(25) Farrugia, L. J. *J. Appl. Crystallogr.* **1999**, *32*, 837.

(26) Becke, A. D. *J. Chem. Phys.* **1993**, *98*, 5648.

(27) Lee, C.; Yang, W.; Parr, R. G. *Phys. Rev. B* **1988**, *37*, 785.

(28) (a) Hay, P. J.; Wadt, W. R. *J. Chem. Phys.* **1995**, *82*, 270. (b) Wadt, W. R.; Hay, P. J. *J. Chem. Phys.* **1995**, *82*, 284. (c) Hay, P. J.; Wadt, W. R. *J. Chem. Phys.* **1995**, *82*, 299.

(29) Frisch, M. J.; Trucks, G. W.; Schlegel, H. B.; Scuseria, G. E.; Robb, M. A.; Cheeseman, J. R.; Zakrzewski, V. G.; Montgomery, J. A.; Stratmann, E.; Burant, J. C.; Dapprich, S.; Millam, J. M.; Daniels, A. D.; Kudin, K. N.; Strain, M. C.; Farkas, O.; Tomasi, J.; Barone, V.; Cossi, M.; Cammi, R.; Mennucci, B.; Pomelli, C.; Adamo, C.; Clifford, S.; Ochterski, J.; Petersson, G. A.; Ayala, P. Y.; Cui, Q.; Morokuma, K.; Malick, D. K.; Rabuk, A. D.; Raghavachari, K.; Foresman, J. B.; Cioslowski, J.; Ortiz, J. V.; Baboul, A. G.; Stefanov, B. B.; Liu, G.; Liashenko, A.; Piskorz, P.; Komaromi, I.; Gomperts, R.; Martin, R. L.; Fox, D. J.; Keith, T.; Al-Laham, M. A.; Peng, C. Y.; Nanayakkara, A.; González, C.; Challacombe, M.; Gill, P. M. W.; Johnson, B.; Chen, W.; Wong, M. W.; Andrés, J. L.; Head-Gordon, M.; Replogle, E. S.; Pople, J. A. *Gaussian 98, revision A.7*; Gaussian Inc., Pittsburgh, PA, 1998.

(30) Mealli, C.; Proserpio, D. M. *J. Chem. Educ.* **1990**, *67*, 399.